Theoretical study of Drug Delivery on Sn (CH₃)₂(N-acetyl-L-cysteinate) with SWCNT

A. Sobhanmanesh[1] and F. Mollaamin[2*]

[1]Ph.D. Student, Science and Research Branch, Islamic Azad University, Tehran, Iran

[2]Department of Chemistry, Science and Research Branch, Islamic Azad University, Tehran, Iran

ABSTRACT

The interaction of anticancer drug Sn $(CH_3)_2$(N-acetyl-L-cysteinate) with carbon nanotube (CNT) is investigated by Quantum chemical ab initio calculations at HF/ (LanL2DZ+STO-3G) and HF/ (LanL2DZ+6-31G) levels in gas phase and solution. The solvent effect is taken into account via the self-consistent reaction field (SCRF) method. Carbon nanotubes can act as a suitable drug delivery vehicle for internalization, transportation and translocation of Sn $(CH_3)_2$(NCA) within biological systems. Thermodynamical analysis indicate that the relative energies (ΔE), enthalpies (ΔH) and free Gibbs energies (ΔG) are negative for Sn $(CH_3)_2$(NCA) –CNT system but the calculated entropies (ΔS) are Positive, suggesting thermodynamic favorability for covalent attachment of Sn $(CH_3)_2$(NCA) into carbon nanotube. Also, the results show that with increasing dielectric constant of solvent the stability of Sn $(CH_3)_2$(NAC) – CNT complex decreases. Furthermore, anisotropic chemical shift tensor ($\Delta\sigma$), total atomic charge and asymmetry parameter (η) have been calculated using the GIAO method, results being compared with CGST data. From the NMR calculations, it can be seen that the NMR ($\Delta\sigma, \eta$) parameters at the sites of nitrogen, oxygen as well as C-2 and C-3 nuclei are significantly influenced by intermolecular hydrogen-bonding interactions but the quantity at the site of S-27 is influenced by nonspecific solute-solvent interaction such as polarizability/polarity.

Keywords: Sn $(CH_3)_2$(N-acetyl-L-cysteinate); NMR parameters; SWNT; Solvent

INTRODUCTION

The chemistry of organotin (IV) has witnessed an increased interest during the last fifty years, owing to their potential biological and industrial applications. However, some organotin (IV) compounds, which were originally modeled on the first tumor-active platinum compound, cisplatin [1], have also found their place among a class of non-platinum chemotherapeutic metallopharmaceuticals exhibiting good antitumor activity [2–6]. In this context, Diorganotin(IV) derivatives and mainly those of dialkyltin(IV) complexes from amino acids ligand are known to possess antimicrobial [7], antimalarial [8], antiproliferative [9], chemotherapeutic [10], radiopharmaceutical [11], insulin-mimetic [12] and fungicidal [13] activities. Further, tin (IV) complexes characterized by the presence of amino acid ligands have proved to be cytotoxic against the breast adenocarcinoma tumor MCF-7, the colon carcinoma [14] and hepatocarcinoma HCC Hep G2 cancer, [15]. In 2010 Girasolo et al. [16] reported the antitumor activity of organotin (IV) complexes containing L-Arginine, Nα-t-Boc-L-Arginine and L-Alanyl-L-Arginine against the Human colon-rectal carcinoma HT29, observing that for all these complexes, cytotoxic activity was higher than that exerted by cisplatin. In 2010 Tzimopoulos et al. [17] reported the results of a screening on wide range of triorganotin aminobenzoates in the K562 myelogenous leukaemia, HeLa cervical cancer and HepG2 hepatocellular carcinoma cells, observing that for triorganotin complexes containing aminobenzoates, cytotoxic activity was better than cisplatin and some triorganotin carboxylates

* Corresponding author: smollaamin@gmail.com

drugs. Furthermore, The cytotoxic activity of Diorganotin(IV) N-acetyl-L-cysteinate complexes towards Human hepatocarcinoma HCC Hep G2 cells were studied by Lorenzo Pellerito and Cristina Prinzivalli in 2010 [15]. In the case at hand, since the discovery of carbon nanotubes (CNTs) in 1991 [18], they have been considered as the ideal material for a variety of applications owing to their unique properties. These properties include their potential biocompatibility in pharmaceutical drug delivery systems and their excellent role as drug carriers with a highly site-selective delivery and sensitivity [19–31]. To accelerate the optimal development of CNT as a new effective drug transporter, it is required to better understand the structural properties of the drug–CNT complex. In this paper we report a computational study of the interaction between Diorganotin (IV) complexes of N-acetyl-L-cysteine (H2NAC; (R)-2-acetamido-3-sulfanylpropanoic acid) whit CNT. We perform a full geometrical, energetical, nuclear magnetic resonance, and vibrational analysis of Sn (CH$_3$)$_2$(NAC) - CNT with different basis set to elucidate the effect of site-specific of these systems. The aim of this study was to investigate the stability of Sn (CH$_3$)$_2$(NAC) – CNT at physiological conditions (temperature, solvent, etc.) and examine the effect of dielectric constant on stability of Sn (CH$_3$)$_2$(NAC) – CNT complex.

COMPUTATIONAL METHODS
The quantum chemical computations in this work were carried out using Gaussian 98 software package [32]. Geometries of Sn(CH$_3$)$_2$(NAC) – CNT complex were optimized in gas phase using the Hartree-Fock method. We used the STO-3G and 6-31G basis sets for all the atoms except for Tin, for which the Lanl2DZ [33-36] basis set was used. Moreover, Vibrational frequencies were calculated in gas phase on the optimized geometries at the same level of theory to obtain the thermal and enthalpy corrections as well as ΔG that is the free energy changes of interaction, and entropy at physiological temperature. The gauge including atomic orbital (GIAO) and Continuous set of gauge transformations (CSGT) methods [37-41] were applied to the optimized structures to achieve anisotropic chemical shift tensor ($\Delta\sigma$) and asymmetry parameter (η). To obtain an estimation of the solvation effects, single point calculations were also conducted on the gas-phase optimized geometries using a Self-Consistent Reaction-Field (SCRF) model [42-45]. Therefore all calculations were repeated in various solvents such as Water ($\varepsilon = 78.39$), Methanol ($\varepsilon = 32.63$) and Ethanol ($\varepsilon = 24.55$).

RESULTS AND DICUSSION
Molecular geometry
The optimized HF/ (LanL2DZ+6-31G) structures for the Sn (CH$_3$)$_2$(NAC) and Sn (CH$_3$)$_2$(NAC) – CNT complex are displayed in Fig. 1. Also, Table 1 depicts the calculated relative energy (kcal/mol) and dipole moments (Debye) in gas phase and solvent phases. From Table 1, we can see that whit increasing dielectric constant (ε) of solvents, the calculated energy of Sn (CH$_3$)$_2$(NAC) – CNT complex decreases. The plot of μ versus $1/\varepsilon$ in both gas phase and in solution is shown in Fig. 2. As can be seen from Fig. 2, whit increasing dielectric constant (ε) of solvents, the dipole moment (μ) of Sn(CH$_3$)$_2$(NAC) – CNT increases.
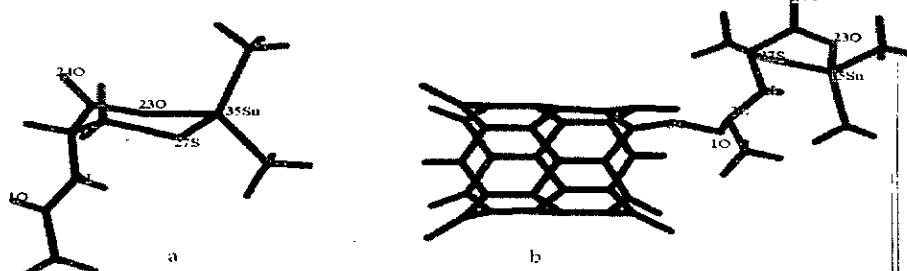

Fig. 1. Optimized geometries of the Sn (CH$_3$)$_2$(NAC) (a) and (Sn (CH$_3$)$_2$(NAC) – CNT complex (b) obtained at the (LanL2DZ÷6-31G) level.

Table.1. Calculated relative energy (kcal/mol) and dipole moments (μ in Debye) of the Sn $(CH_3)_2(NAC)$ – CNT complex obtained at the (LanL2DZ+STO-3G) and (LanL2DZ+6-31G) levels

	Gas phase	Water	Methanol	Ethanol
Basis set	E (kcal/mol)			
Sto-3G	-1528418.194926134883	-1528361.926661349704	-1528365.446429708648	-1528364.908184099206
6-31G	-1546711.056411545919	-1546663.537831896343	-1546664.499741357760	-1546664.546496487819
Basis set	μ (Debye)			
Sto-3G	1.9913	24.5881	25.0154	24.9129
6-31G	3.9221	25.2208	25.9544	25.8441
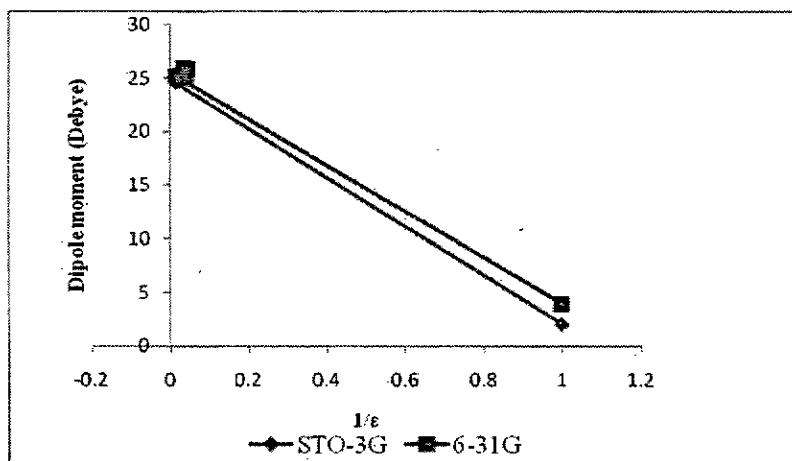
Fig. 2. Plot of the μ (Debye) versus the $1/\varepsilon$, obtain from the (LanL2DZ+STO-3G) and (LanL2DZ+6-31G) calculations for Sn $(CH_3)_2(NAC)$ – CNT Complex.

Calculated NMR parameters

The calculated anisotropic chemical shift tensor ($\Delta\sigma$), total atomic charge and asymmetry parameter (η) for selected atoms of Sn $(CH_3)_2(NAC)$ – CNT complex in both gas phase and in solution at GIAO and CSGT methods are specified in Table 2. The graphs of calculated anisotropic chemical shift tensor ($\Delta\sigma$), asymmetry parameter (η) and total atomic charge versus the atomic number are also drawn in Figs. 3a-c respectively. As shown in Fig.3, the Sn-35 nucleus has maximum total atomic charge and low $\Delta\sigma$ values in both gas phase and in solution, meaning the relative chemical shift at the site of Sn-35 is predominantly governed by local diamagnetic shielding

term (σ^d). Further, Tin atom has large amounts of asymmetry parameter (η) in both gas phase and in solution (see Fig.3b). The results in solution indicate that the anisotropic chemical shift tensor ($\Delta\sigma$) of Sn-35 decreases in the order Gas Phase > Ethanol > Methanol >Water and also asymmetry parameter (η) at the site of Sn-35 decreases in the order Ethanol > Methanol >Water >Gas Phase (see Fig. 3a and Fig. 3b). The observed changes can be due to presence of the solvent molecule in the Tin inner coordination sphere. Since Sulfur atom possess negative and Tin atom has positive charges (see Fig.3c), this difference in the charges leads to a larger anisotropic chemical shift tensor ($\Delta\sigma$) for the sulfur

atom (see Fig.3a). The results in Fig.3a show that, with increase of dielectric constant from gas phase to water, the $\Delta\sigma$ at the site of sulfur atom decreases. In addition, Fig.3b indicates that asymmetry parameter (η) of S-27 in solution are larger than gas phase. The observed effect is probably due to the nonspecific solute-solvent interaction (such as polarizability/polarity) at the site of S-27 nucleus. Since N-5 is more negative than S-27 (see Fig.3c), N-5 nucleus has the lower $\Delta\sigma$ value than the S-27 nucleus (see Fig.3a). Also, Fig.3b shows that η for N-5 has minimum value. The results in solution show that with increasing dielectric constant of solvent, the $\Delta\sigma$ and η values of N-5 atom decrease (see Fig.3a and Fig.3b). It can be said that the NMR ($\Delta\sigma$, η) parameters at the site of N-5 nucleus are significantly influenced by intermolecular hydrogen-bonding interactions. Since carbon atoms (C-2 and C-3) are more positive than N-5 (see Fig.3c), the $\Delta\sigma$ values at the sites of C-2 and C-3 are greater than the N-5 nucleus (see Fig.3a). As shown in Fig.3b, the η values for the carbon atoms are larger than nitrogen atom. The results in solution show that with increasing dielectric constant of solvent, the $\Delta\sigma$ and η values of C-2 atom increase (see Fig.3a and Fig.3b). Moreover, with increasing dielectric constant of solvent, the $\Delta\sigma$ value at the site of C-3 increases (see Fig.3a). The observed effect is probably due to the intermolecular hydrogen- bonding interactions at the sites of carbon nuclei. The results in Fig 3b indicate that the η values of C-3 are larger than that of C-2. Also, since the $\Delta\sigma$ constants for the C-2 are larger than $\Delta\sigma$ values for the C-3 (see Fig.3a); it seems that the C-3 is more shielded than the C-2 nucleus. Since the electrostatic properties are mainly dependent on the electronic densities at the sites of nuclei, Oxygen plays a significantly different role among the other nuclei (S, C, Sn and N atoms). Total atomic charge for O-23 nucleus is minimum

meaning O-23 nucleus has maximum electron shielding (see Fig.3c). This leads to a minimum anisotropic chemical shift tensor ($\Delta\sigma$) at the site of O-23 atom (see Fig.3a). Also, Fig.3b shows that O-23 has small amounts of η in both gas phase and solution. The results in Fig.3a indicate that, the anisotropic chemical shift tensor ($\Delta\sigma$) at the site of O-23 decreases in the order Methanol > Ethanol> Water> Gas Phase. Meaning O-23 nucleus has maximum electron shielding in gas phase but the quantity is minimum in Methanol. In addition, Fig.3b indicates that asymmetry parameter (η) of O-23 in solution are larger than gas phase. In this regard, it seems that the NMR ($\Delta\sigma$, η) parameters at the site of O-23 nucleus are significantly influenced by intermolecular hydrogen-bonding interactions. On the other hand, Fig.3c shows that O-23 posses more negative than O-24 nucleus. This difference in the total atomic charge values lead to a maximum anisotropic chemical shift tensor ($\Delta\sigma$) at the site of O-24 atom (see Fig.3a). The results in solution indicate that the anisotropic chemical shift tensor ($\Delta\sigma$) of O-24 decreases in the order Ethanol > Methanol> Water> Gas Phase. Meaning O-24 nucleus has maximum electron shielding in gas phase but the quantity is minimum in Methanol. In addition, Fig.3b indicates that asymmetry parameter (η) of O-24 in gas phase are larger than solution. It can be said that the NMR ($\Delta\sigma$, η) parameters at the site of O-24 nucleus are significantly influenced by intermolecular hydrogen-bonding interactions. As shown in Fig.3b, O-1 nucleus has large amounts of anisotropic chemical shift tensor ($\Delta\sigma$) in gas phase but the quantity is smaller in Methanol. Moreover, with increase of dielectric constant from gas phase to water, the asymmetry parameter (η) at the site of O-1 decreases (see Fig.3b). The observed effect is probably due to the intermolecular hydrogen- bonding interactions at the site of O-1 nucleus.

Table.2. Calculated NMR parameters of Sn (CH₃)ᵦ(NAC) – CNT complex in gas phase and various solvents at GIAO and CSGT methods

|	Δσ				η				Charge			
	GIAO		CSGT		GIAO		CSGT		GIAO		CSGT	
	HF/STO-3G	HF/6-31G	HF/STO-3G	HF/6-31G	HF/STO-3G	HF/6-31G	HF/STO-3G	HF/6-31G	HF/STO-3G	HF/6-31G	HF/STO-3G	HF/6-31G
Gas phase												
atoms												
1O	133.27625	162.2032	151.30455	175.7776	0.76422159395	0.9834975563	0.9300166452	0.9347407944	-0.206606	-0.665951	-0.206606	-0.665951
5N	-57.2367	66.76195	-22.9373	56.26365	0.6262887273	0.3252156915	0.8939214596	0.2662313945	-0.334198	-0.789626	-0.334198	-0.789626
23O	-349.1178	-301.8081	-248.5697	-302.31045	0.3139183965	0.1528865527	0.3507544062	0.1448529152	-0.378221	-0.930993	-0.378221	-0.930993
24O	893.6313	777.985	648.91945	681.3507	0.4924870021	0.3582897897	0.3652486171	0.3748171096	-0.255457	-0.524892	-0.255457	-0.524892
27S	393.09555	153.6641	188.15355	185.67265	0.2234956615	0.3642016438	0.8304278606	0.0889751158	0.036317	-0.174392	0.036317	-0.174392
35Sn	3.307	4.26845	5.98665	5.06225	0.4298090443	0.1535352825	0.6075768585	0.4750800047	0.625426	1.679188	0.625426	1.679188
2C	38.1788	49.1969	20.75265	52.48415	0.4565131126	0.087255586	0.3432501391	0.3628213115	0.238337	0.549121	0.238337	0.549121
3C	-102.699	-126.6157	-105.86055	-134.22655	0.8072211024	0.7654734896	0.7791840303	0.7699297307	0.135517	0.405128	0.135517	0.405128
Water												
atoms												
1O	-298.01245	-300.86675	-288.25255	-307.59315	0.8861895054	0.8026426653	0.4601752734	0.6260586427	-0.205436	-0.776383	-0.205436	-0.776383
5N	-133.43445	-215.8869	-145.21055	-226.2453	0.0537083938	0.0386257804	0.1667678990	0.1421837271	-0.304099	-0.860286	-0.304099	-0.860286
23O	-207.47025	-222.6352	-181.6076	-230.7312	0.9823661464	0.1573214484	0.5406366640	0.1036517818	-0.369772	-0.919359	-0.369772	-0.919359
24O	909.353	814.2384	694.5349	728.01665	0.4698565062	0.3953785525	0.2887677574	0.3665353921	-0.221098	-0.489641	-0.221098	-0.489641
27S	284.85405	129.7666	-217.006	-163.41745	0.3712559115	0.83366411	0.7676163867	0.9306107949	0.032035	-0.203277	0.032035	-0.203277
35Sn	-4.42025	3.4626	4.5463	3.53725	0.8699267001	0.2932767284	0.7790425286	0.8262657959	0.607104	1.598030	0.607104	1.598030
2C	148.06185	187.45305	122.6329	192.74475	0.2728464489	0.6484607745	0.4392620417	0.4653239582	0.410397	0.914918	0.410397	0.914918
3C	83.1298	-99.01685	77.66165	-103.3895	0.8494241238	0.8790887000	0.9861108965	0.8794843187	0.055560	0.190564	0.055560	0.190564
Methanol												
atoms												
1O	306.6367	315.3896	-288.51055	-310.52655	0.9104417523	0.8603493679	0.6244042460	0.8928584367	-0.198399	-0.750570	-0.198399	-0.750570
5N	306.6367	315.3896	-288.51055	-310.52655	0.9104417523	0.8603493679	0.6244042460	0.8928584367	-0.198399	-0.750570	-0.198399	-0.750570
23O	-132.8056	-213.95105	-145.5225	-223.4479	0.0363711935	0.0396896953	0.1742039890	0.1449934984	-0.305193	-0.868067	-0.051359	-0.411311
24O	-204.55385	-220.50135	-179.9908	-227.8303	0.9964031467	0.1451753016	0.5623685870	0.1046449638	-0.372293	-0.922565	-0.372293	-0.922565
27S	916.5669	823.7247	701.08365	735.48065	0.4710625050	0.3917073264	0.2935350867	0.3588210892	-0.218476	-0.489386	-0.218476	-0.489386
35Sn	289.6761	129.9141	-222.21485	-161.31185	0.3427158816	0.8774959761	0.7697477845	0.9393674238	0.031227	-0.205365	0.031227	-0.205365
2C	-4.5373	3.61365	4.408	3.58385	0.9161955767	0.3358515628	0.8490148705	0.8536330152	0.603715	1.593134	0.603715	1.593134
3C	146.5689	182.3604	124.0064	189.05055	0.22265091707	0.5901593767	0.3927935948	0.3924688396	0.408575	0.924082	0.408575	0.924082
Ethanol												
atoms												
1O	307.21795	316.009	-287.6853	-309.91085	0.9031506942	0.8526258978	0.3156621141	0.8997445393	-0.198587	-0.750865	-0.198587	-0.750865
5N	-132.753	-213.9204	-145.47475	-223.45565	0.0403199927	0.0398938109	0.1723692065	0.1429914936	-0.305292	-0.868087	-0.305292	-0.868087
23O	204.0473	-220.72555	-180.20645	-228.24925	0.9989796488	0.1431929508	0.5601834895	0.1014187119	-0.372438	-0.922664	-0.372438	-0.922664
24O	916.32285	823.794	701.02135	735.5615	0.4701214751	0.3901241086	0.2919841676	0.3569444809	-0.218414	-0.489307	-0.218414	-0.489307
27S	290.08825	129.9081	-221.7231	-161.15845	0.3402769087	0.8765896814	0.7764441323	0.9438332449	0.031256	-0.204437	0.031256	-0.204437
35Sn	-4.55265	3.6277	4.40665	3.5843	0.9132812757	0.3427744469	0.8460700548	0.8492634750	0.603779	1.593023	0.603779	1.593023
2C	146.43065	182.46825	123.8593	189.1353	0.2224914054	0.5933199337	0.3917968243	0.3946460549	0.408701	0.923818	0.408701	0.923818
3C	-85.53375	-105.47775	-85.16655	-111.64375	0.7982480599	0.5675903211	0.7803715190	0.6458768870	0.038610	0.176795	0.038610	0.176795
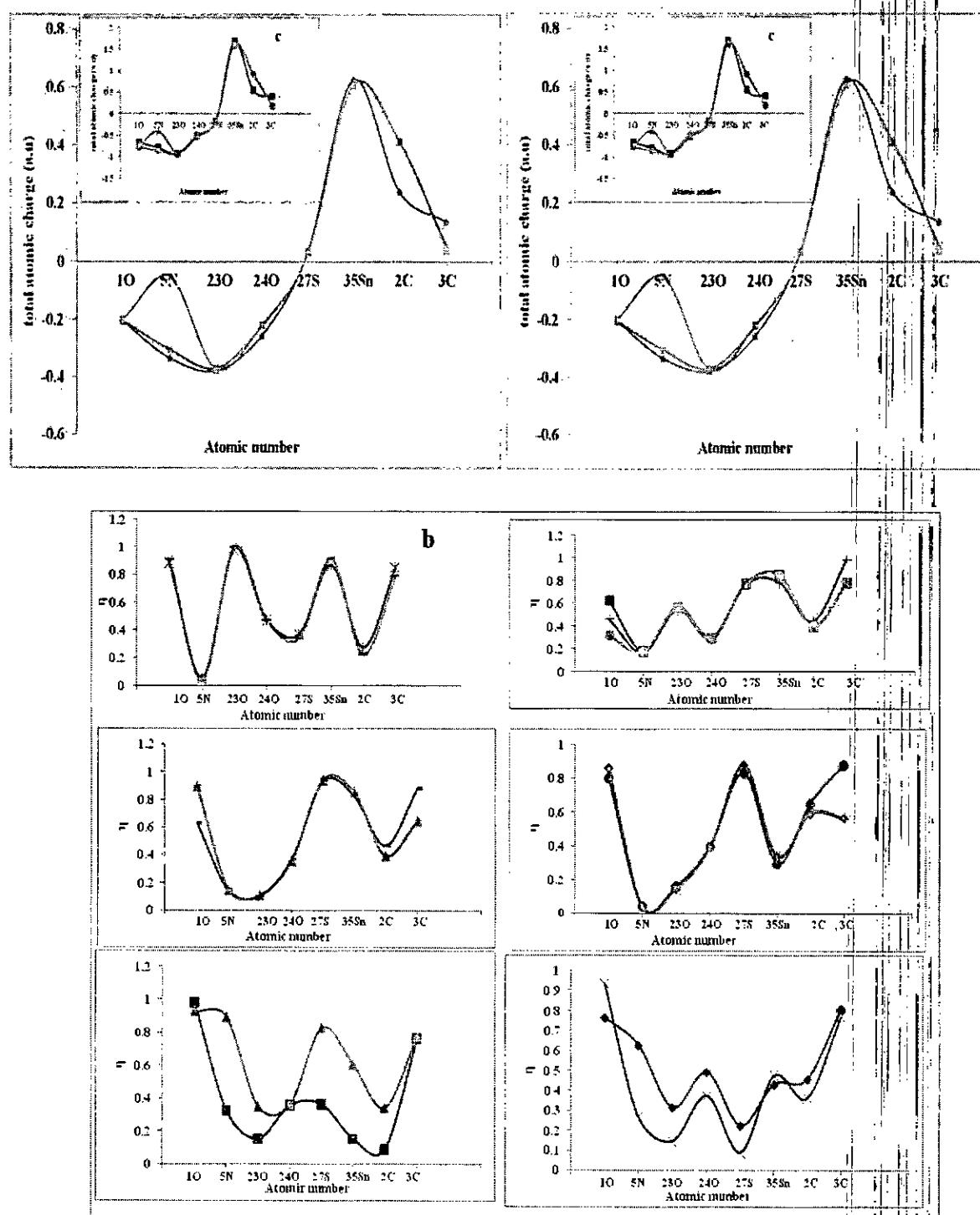
Fig. 3. Graphs of the $\Delta\sigma$(ppm) versus atomic number (a), η versus atomic number (b), total atomic charge (a.u) versus atomic number (c), for selected atoms of $Sn(CH_3)_2(NAC)$ – CNT complex in both gas phase and in solution obtain from the GIAO and CSGT methods.

GIAO/HF/STO-3G/GAS	GIAO/HF/6-31G/GAS	CSGT/HF/STO-3G/GAS	CSGT/HF/6-31G/GAS
GIAO/HF/STO-3G/WATER	GIAO/HF/6-31G/WATER	CSGT/HF/STO-3G/WATER	CSGT/HF/6-31G/WATER
GIAO/HF/STO-3G/METANOL	GIAO/HF/6-31G/METANOL	CSGT/HF/STO-3G/METANOL	CSGT/HF/6-31G/METANOL
GIAO/HF/STO-3G/ETHANOL	GIAO/HF/6-31G/ETHANOL	CSGT/HF/STO-3G/ETHANOL	CSGT/HF/6-31G/ETHANOL

Thermodynamic analysis

Table 3 displays the calculated relative energies (ΔE), enthalpies (ΔH), and free Gibbs energies (ΔG) as well as entropy (ΔS) in both gas phase and in solution, for $Sn(CH_3)_2(NAC)$ – CNT complex at the physiological temperature. In addition, the plots of calculated relative energies (ΔE), enthalpies (ΔH), and entropy (ΔS) as well as free Gibbs energies (ΔG) versus the physiological temperature are drown in Figs. 4a-d respectively. From Table 3 and Figs. 4 it can be seen that $Sn(CH_3)_2(NAC)$ – CNT complex has negative values of relative energies (ΔE),

enthalpies (ΔH) and free Gibbs energies (ΔG) in both gas phase and in solution. Also, our results in Table 3 and Figs. 4c show that entropy (ΔS) for $Sn (CH_3)_2(NAC)$ – CNT system has Positive values. These observations can be related to the structural stability of the $Sn (CH_3)_2(NAC)$ – CNT in both gas phase and in solution. the results in Figs. 4 show that, with increase of dielectric constant from gas phase to water, the stability of $Sn(CH_3)_2(NAC)$ – CNT complex decreases.

Table. 3. Calculated relative electronic energies (kcal/mol), enthalpies (kcal/mol), free Gibbs energies (kcal/mol) and entropies (kcal/molK) in both gas phase and in solution, for the $Sn(CH_3)_2(NAC)$ – CNT complex obtained at the level of HF/ (LanL2DZ+STO-3G)

Temprature (K)	Gas phase	Water	Ethanol	Methanol
		ΔE(kcal/mol)		
298.15	-1528088.69709835099	-1528012.26240660171	-1528015.4118361785	-1528015.2235857555
300.15	-1528088.40091768547	-1528011.96308842914	-1528015.10938049888	-1528014.92050257447
302.15	-1528088.10285451572	-1528011.66188775234	-1528014.80441481362	-1528014.61616439062
304.15	-1528087.80290884174	-1528011.35943207272	-1528014.49882162695	-1528014.31057120395
306.15	-1528087.50170816494	-1528011.05572139028	-1528014.19134593605	-1528014.00309551305
308.15	-1528087.19925248532	-1528010.75012820361	-1528013.88198774092	-1528013.69373731792
310.15	-1528086.89491430147	-1528010.44265251271	-1528013.57137454297	-1528013.38312411997
312.15	-1528086.5893211148	-1528010.13392181899	-1528013.2595063422	-1528013.0712559192
313.15	-1528086.43558326935	-1528009.97892897072	-1528013.1026309897	-1528012.9143805667
Temprature (K)		ΔH(kcal/mol)		
298.15	-1528088.10473701995	-1528011.66941776926	-1528014.81947484746	-1528014.63122442446
300.15	-1528087.80416384456	-1528011.36633458823	-1528014.51262665797	-1528014.32437623497
302.15	-1528087.50233566635	-1528011.06136890297	-1528014.20452346566	-1528014.01627304266
304.15	-1528087.1986249839I	-1528010.75514821489	-1528013.89453776912	-1528013.70628734612
306.15	-1528086.89365929865	-1528010.44704502258	-1528013.58266956835	-1528013.39441914535
308.15	-1528086.58681110916	-1528010.13768682745	-1528013.27017386617	-1528013.08192344317
310.15	-1528086.27870791685	-1528009.82644612809	-1528012.95516815835	-1528012.76691773535
312.15	-1528085.96872222031	-1528009.51395042591	-1528012.63890744771	-1528012.45128452612
313.15	-1528085.81310187063	-1528009.35707507341	-1528012.48077709239	-1528012.29252666939
Temprature (K)		ΔG(kcal/mol)		
298.15	-1528156.53313827904	-1528084.24372084422	-1528087.32287026309	-1528086.34020305503
300.15	-1528156.99309681257	-1528084.7319169412	-1528087.80981135725	-1528086.82212413791
302.15	-1528157.45493785033	-1528085.221368041	-1528088.29926245705	-1528087.30655522643
304.15	-1528157.91866139232	-1528085.71332914644	-1528088.79059606108	-1528087.79224131777
306.15	-1528158.38489493995	-1528086.20717275611	-1528089.28443967075	-1528088.28043741475
308.15	-1528158.85301099181	-1528086.70352637142	-1528089.78016578465	-1528088.77114351737
310.15	-1528159.3230095479	-1528087.20113498955	-1528090.27777440278	-1528089.26310462281
312.15	-1528159.79489060822	-1528087.70125361332	-1528090.77726552514	-1528089.75757573389
313.15	-1528160.0320861412	-1528087.95162667591	-1528097.5783248473	-1528090.00543879084
Temprature (K)		ΔS(kcal/molK)		
298.15	0.229512	0.243418	0.24318	0.240517
300.15	0.230516	0.244432	0.244206	0.241542
302.15	0.231519	0.245444	0.24523	0.242566
304.15	0.23252	0.246455	0.246252	0.243588
306.15	0.23352	0.247464	0.247272	0.244609
308.15	0.234519	0.248472	0.248292	0.245628
310.15	0.235516	0.249479	0.249309	0.246645
312.15	0.236512	0.250483	0.250325	0.247661
313.15	0.237009	0.250985	0.250833	0.248169
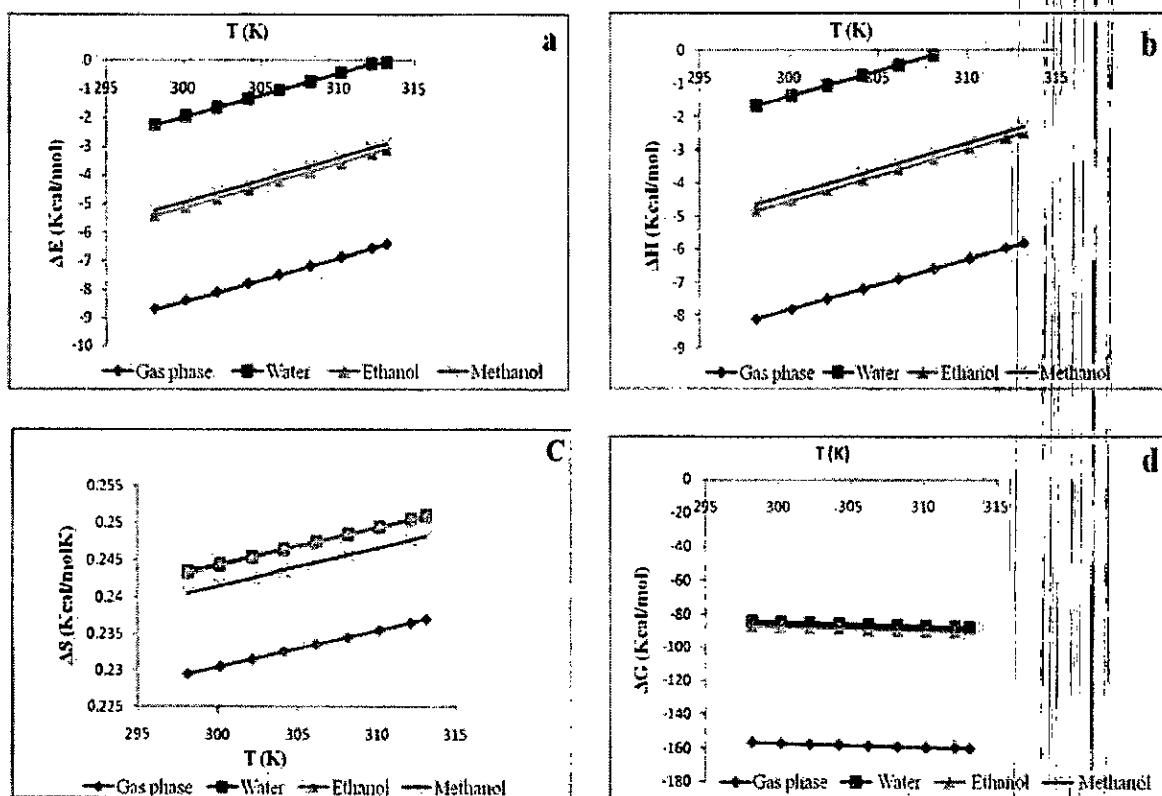
Fig. 4. Plots of the ΔE (kcal/mol) versus the T (K) (a), ΔH (kcal/mol) versus the T (K) (b), ΔS (kcal/molK) versus the T (K) (c), ΔG (kcal/mol) versus the T (K) (d), for $Sn(CH_3)_2(NAC)$ – CNT Complex in both gas phase and in solution, obtain from the (LanL2DZ+STO-3G) calculations .

CONCLUSION

1- O-24 has maximum anisotropic chemical shift tensor ($\Delta\sigma$) constant but the quantity in the O-23 and O-1 nuclei are minimum.

2- Sn-35 has maximum total atomic charge but the quantity in the O-23 nucleus is minimum.

3- The NMR ($\Delta\sigma, \eta$) parameters at the sites of nitrogen, oxygen as well as C-2 and C-3 are significantly influenced by intermolecular hydrogen- bonding interactions but the quantity at the site of S-27 is influenced by nonspecific solute-solvent interaction such as polarizability/polarity.

4- The thermodynamic analysis show that with increase of dielectric constant from gas phase to water, the stability of $Sn(CH_3)_2(NAC)$ – CNT complex decreases.

REFERENCES

[1] C.F.J. Bamard, Platin. Met. Rev. 33 (1989) 162–167.

[2] A.J. Crowe, P.J. Smith, Chem. Ind. (Lond.) (1980) 200–201.

[3] A.K. Saxena, F. Huber, Coord. Chem. Rev. 95 (1989) 109–123.

[4] M. Gielen, Coord. Chem. Rev. 151 (1996) 41–51.

[5] M.J. Clarke, F. Zhu, D.R. Frasca, Chem. Rev. 99 (1999) 2511–2534.

[6] M. Nath, S. Pokharia, R. Yadav, Coord. Chem. Rev. 215 (2001) 99–149 and references therein.

[7] G. Plesch, C. Friebel, O. Svajlenova, J. Kratsmar-Smogrovic, D. Mlynarcik, Inorg. Chim. Acta 151 (2) (1988) 139–143.

[8] D.E. Goldberg, V. Sharma, A. Oksman, I.Y. Gluzman, T.E. Wellems, D. Piwnica-Worms, J. Biol. Chem. 272 (10) (1997) 6567–6572.

[9] P. Kpf-Maier, H. Kpf, Chem. Rev. 87 (5) (1987) 1137–1152.

[10] M.Z. Wang, Z. Meng, B. Liu, G. Cai, C. Zhang, X. Wang, Inorg. Chem. Commun. 8(4) (2005) 368–371.

[11] M.Z. Wang, Z. Meng, J. Fu, Appl. Radiat. Isot. 64 (2) (2006) 235–240.

[12] J.C. Pessoa, I. Covaco, I. Correia, M.T. Duarte, R. D, Gillard, R.T. Henriques, F.J. Higes, C. Madeira, I. Tomaz, Inorg. Chim. Acta 293 (1) (1999) 1–11.

[13] G. Eng, D. Whalen, Y.Z. Zhang, A. Kirksey, M. Otieno, L.E. Khoo, B.D. James, Appl. Organomet. Chem. 10 (7) (1996) 501–503.

[14] M. Gielen, Coord. Chem. Rev. 151 (1996) 41–51.

[15] L. Pellerito, C. Prinzivalli, G. Casella, T. Fiore, O. Pellerito, M. Giuliano, M. Scopelliti , C. Pellerito, J.Inorg. Biochem. 104 (2010) 750–758.

[16] M. A. Girasolo, S. Rubino, P. Portanova, G. Calvaruso, G. Ruisi, G. Stocco, J.Organom. Chem. 695 (2010) 609–618.

[17] D. Tzimopoulos, I. Sanidas, A.C. Varvogli, A. Czapik, M. Gdaniec, E. Nikolakaki, P. D. Akrivos , J. Inorg. Biochem. 104 (2010) 423–430.

[18] S. Iijima, Helical microtubules of graphitic carbon, Nature 354 (1991) 56–58.

[19] Bianco, K. Kostarelos, C.D. Partidos, M. Prato, Biomedical applications of functionalised carbon nanotubes, Chem. Commun. (2005) 571–577.

[20] S.K. Smart, A.I. Cassady, G.Q. Lu, D.J. Martin, The biocompatibility of carbon nanotubes, Carbon 44 (2006) 1034–1047.

[21] A.M. Popov, Y.E. Lozovik, S. Fiorito, L.H. Yahia, Biocompatibility and applications of carbon nanotubes in medical nanorobots, Int. J. Nanomed. 2 (2007) 361–372.

[22] S. Banerjee, T. Hemraj-Benny, S.S. Wong, Covalent surface chemistry of singlewalled carbon nanotubes, Adv. Mater. 17 (2005) 17–29.

[23] G. Pastorin, W. Wu, S.B. Wieckowski, J.-P. Briand, K. Kostarelos, M. Prato, et al.,Double functionalisation of carbon nanotubes for multimodal drug delivery, Chem. Commun. (2006) 1182–1184.

[24] C. Klumpp, K. Kostarelos, M. Prato, A. Bianco, Functionalized carbon nanotubes as emerging nanovectors for the delivery of therapeutics, Biochim. Biophys. Acta: Biomembr. 1758 (2006) 404–412.

[25] K. Kostarelos, L. Lacerda, G. Pastorin, et al., Cellular uptake of functionalized carbon nanotubes is independent of functional group and cell type, Nat. Nanotechnol. 2 (2007) 108–113.

[26] V. Raffa, G. Ciofani, S. Nitodas, T. Karachalios, D. D'Alessandro, M. Masini, et al., Can the properties of carbon nanotubes influence their internalization by living cells? Carbon 46 (2008) 1600–1610.

[27] X. Zhang, L. Meng, Q. Lu, Z. Fei, P.J. Dyson, Targeted delivery and controlled release of doxorubicin to cancer cells using modified single wall carbon nanotubes, Biomaterials 30 (2009) 6041–6047.

[28] Lee. V. S., Nimmanpipug. P, Mollaamin. F, Kungwan. N, Thanasanvorakun. S, and M. Monajjemi Investigation of Single Wall Carbon Nanotubes Electrical Properties and Normal Mode Analysis: Dielectric Effects Russian Journal of Physical Chemistry A, 2009, Vol. 83, No. 13, pp. 2288–2296.

[29] M. Monajjemi, L. Mahdavian, F. Mollaamin and M. Khaleghian

[30] Interaction of Na, Mg, Al, Si with Carbon Nanotube (CNT): NMR and IR Study Russian Journal of Inorganic Chemistry, 2009, Vol. 54, No. 9, pp. 1465–1473.

[31] M. Monajjemi, L. Mahdavian, F.Mollaamin. Characterization of nanocrystalline cylicon germanium film and nanotube in adsoption gas by monte carlo and langevin dynamic simulation Bull. Chem. Soc. Ethiop, 2008, 22(2), 1-10.

[32] H. Aghaie, M. R. Gholami, M. Monajjemi, M. D. Ganji. Electron transport phenomenon simulation through the carborane nano-molecular wire Physica E: Low-Dimensional Systems and Nanostructures 40 (9), pp. 2965-2972, 2008.

[33] GAUSSIAN 03, Revision C.02: M.J. Frisch et al. Gaussian Inc., Wallingford CT, 2004.

[34] Ariafard, M.D. Asli, H. Aghabozorg, H. Aghabozorg, M. Monajjemi. Theoretical studies of rotational barriers of dithiocarbamate ligands in the square planar complexes TM (L) (L ') (H (2) dtc)

(TM = Ir, Rh) J. of Molecular Structure-Theochem 636: 49-56 SEP 30 2003.

[35] Ariafard, R. Fazaeli, HR. Aghabozorg, M. Monajjemi. DFT study of metal-tetrahydroborato ligand interactions in [Ti (CO) (4) (BH4)] J. of Molecular Structure-Theochem 625: 305- 314 MAY 5 2003.

[36] P.J. Hay, W.R. Wadt, J. Chem. Phys. 82 (1985) 270.

[37] W.R. Wadt, P.J. Hay, J. Chem. Phys. 82 (1985) 284.

[38] Wrackmeyer, Annu. Rep. NMR Spectrosc. 16 (1985) 73–186.

[39] R. Ditchfield, J. Chem. Phys. 56 (1972) 5688–5692.

[40] P. Pulay, K. Wolinski, J.F. Hinton, J. Am. Chem. Soc. 112 (1990) 8251–8260.

[41] M. Monajjemi, S. Afsharnezhad, M.R. Jaafari, S. Mirdamadi, F. Mollaamin, H. Monajemi. Investigation of energy and NMR isotropic shift on the internal rotation Barrier of Θ4 dihedral angle of DLPC: A GIAO study Chemistry 17(1), pp. 55-69, 2008.

[42] T.A. Keith, R.F.W. Bader, Chem. Phys. Lett. 210 (1993) 223.

[43] M. Miertus, E. Scrocco, J. Tomasi, Chem. Phys. 55 (1981) 117–129.

[44] S. Miertus, J. Tomasi, Chem. Phys. 65 (1982) 239–252.

[45] M. Monajjemi, B. Chahkandi. Theoretical investigation of hydrogen bonding in Watson-Crick, Hoogestein and their reversed and other models: comparison and analysis for configurations of adenine-thymine base pairs in 9 models J. of Molecular Structure-Theochem. 714 (1): 43-60 JAN 31 2005.

[46] R. Fazaeli, M. Monajjemi, F. Ataherian. Solvent effects on relative stabilities and N-14 NMR shielding of cytosine tautomers: continuous set of gauge transformation calculation using polarizable continuum model J. of Molecular Structure-Theochem 581: 51-58 APR 5 2002.